

# ChemComm

Chemical Communications

Accepted Manuscript

This article can be cited before page numbers have been issued, to do this please use: Q. Wu, Z. Liu, Q. Su, P. Ju, X. Li, G. Li and B. Yang, *Chem. Commun.*, 2019, DOI: 10.1039/C9CC07661A.



This is an Accepted Manuscript, which has been through the Royal Society of Chemistry peer review process and has been accepted for publication.

Accepted Manuscripts are published online shortly after acceptance, before technical editing, formatting and proof reading. Using this free service, authors can make their results available to the community, in citable form, before we publish the edited article. We will replace this Accepted Manuscript with the edited and formatted Advance Article as soon as it is available.

You can find more information about Accepted Manuscripts in the [Information for Authors](#).

Please note that technical editing may introduce minor changes to the text and/or graphics, which may alter content. The journal's standard [Terms & Conditions](#) and the [Ethical guidelines](#) still apply. In no event shall the Royal Society of Chemistry be held responsible for any errors or omissions in this Accepted Manuscript or any consequences arising from the use of any information it contains.

## COMMUNICATION

## A hydrophilic covalent organic framework for photocatalytic oxidation of benzylamine in water

Ziqian Liu,<sup>a</sup> Qing Su,<sup>\*a</sup> Pengyao Ju,<sup>a</sup> Xiaodong Li,<sup>a</sup> Guanghua Li,<sup>b</sup> Qiaolin Wu,<sup>\*a</sup> and Bing Yang<sup>\*c</sup>Received 00th January 20xx,  
Accepted 00th January 20xx

DOI: 10.1039/x0xx00000x

**The highly hydrophilic COF material (TFPT-BMTH) was constructed by pore surface functionalizing strategy, and exhibited excellent porosity, high crystallinity, and good thermal and chemical stability. The resulting COF exhibits significant catalytic activity and recyclability together with environmental benignity in photocatalytic oxidation of benzylamine in water under ambient conditions.**

COFs have emerged an exciting class of crystalline porous polymers connected by building blocks through covalent bonds in a two-dimensional (2D) or three-dimensional (3D) direction,<sup>1,2</sup> and therefore attracted intensive research interests for a range of applications including gas adsorption,<sup>3</sup> chemical sensing,<sup>4</sup> photoconductivity,<sup>5</sup> energy storage,<sup>6</sup> and catalysis.<sup>7</sup> Considering high surface area, extended  $\pi$ -conjugated framework and the layered stacking structure, COFs have provided ideal channels that enable exciton migration and charge separation.<sup>8</sup> In this regard, COFs have been explored with prominent light harvesting capability and tunable band gap, and therefore emerged as photoactive materials for light-driven organic transformations.<sup>9</sup> For example, our group developed the hydrazone-based COF as highly active photocatalyst in cross-dehydrogenative coupling (CDC) reactions.<sup>10</sup> Similar hydrazone-based COFs were previously reported to show light-induced hydrogen evolution in the presence of Pt.<sup>11</sup> The imine-based COFs were also employed as metal-free photocatalysts to show remarkable catalytic activity in visible light-mediated CDC reactions.<sup>12</sup> However, it is worth noting that some photoactive COFs have been found to hardly keep unchanged after recyclability tests.<sup>13</sup> Therefore, it remains a great challenge to explore new COFs systems that are highly stable, and highly active in heterogeneous photocatalysis.

Inspired by natural photosynthesis, we have been interested in developing COF photocatalysts, which could serve as environmentally friendly alternative, similar to light-responsive Metal Organic Frameworks (MOFs).<sup>14</sup> Up to now, the reported photocatalytic tests have been usually carried out in organic solvents or organic co-solvents.<sup>9,15</sup> From the viewpoint of sustainability and environment, it is highly desirable to develop hydrophilic photocatalyst systems with high catalytic performance, minimum environmental impact and energy consumption. Based on the excellent photophysical properties, Triazine-based molecules are hence employed as a building blocks to construct photoactive COFs,<sup>10,11</sup> featuring the high surface area and high crystallinity. Herein, we report a highly hydrophilic hydrazone-based COF from TFPT and BMTH building units. The 2-methoxyethoxy groups are periodically appended on the channel walls, which reinforces interlayer interactions by the effective control over the stacking model and stability of COF, and also enhances surface hydrophilicity with the increase in ether content. As compared with other imine or boronate-based COFs,<sup>12</sup> the obtained **TFPT-BMTH** should exhibit some advantages, such as high hydrophilicity, unprecedented stability and recyclability, together with aqueous photocatalytic applications. The resulting COF was employed to achieve excellent photocatalytic activity for oxidation of benzylamine in water. Selective oxidative coupling of amines to imines is attractive due to the use of imines for the synthesis of pharmaceutically and biologically active compounds.<sup>16</sup> Meanwhile, the COF material **TFPT-BMTH** benefited from strong covalent linkages and strengthened interlayer interactions, and thus showed unprecedented stability and recyclability in the cycling tests with retaining its activity and crystallinity after five successive runs. To our knowledge, there are a very few examples to achieve aqueous photocatalytic organic transformations using COF photocatalyst.<sup>13</sup>

The **TFPT-BMTH** with incorporating 2-methoxyethoxy groups into the channel walls was constructed from the condensation reaction of TFPT with BMTH by organic acid catalysis (scheme S1). The resulting **TFPT-BMTH** was first characterized by power X-ray diffraction (PXRD) analysis. The observed PXRD pattern showed the most intensive peak at 2.3° and a weak diffraction peak at 4.7°, which corresponded

<sup>a</sup> College of chemistry, Jilin University, 2699 Qianjin Street, Changchun 130012, P. R. China

<sup>b</sup> State Key Laboratory of Inorganic Synthesis and Preparative Chemistry, Jilin University, 2699 Qianjin Street, Changchun 130012, P. R. China

<sup>c</sup> State Key Laboratory of Supramolecular Structure and Materials, Jilin University, 2699 Qianjin Street, Changchun 130012, P. R. China

† Corresponding author mails: suqing@jlu.edu.cn; wuql@jlu.edu.cn.  
Electronic Supplementary Information (ESI) available: [details of any supplementary information available should be included here]. See DOI: 10.1039/x0xx00000x

to the reflection from the plane (100) and (110),<sup>17</sup> respectively (Fig. 1a), and also indicated the high crystallinity of the obtained COF.

The permanent porosity of **TFPT-BMTH** were determined by nitrogen adsorption measurements at 77 K. As shown in Fig. 1b, the nitrogen adsorption curves of **TFPT-BMTH** exhibited a type IV sorption isotherm with a rapid uptake at  $P/P_0 < 0.1$  and a sharp step increase in the curve in the relative pressure range of 0.2–0.4 ( $P/P_0$ ) (Fig. 1b).<sup>18</sup> The BET surface area and total pore volume are estimated to be  $603 \text{ m}^2\text{g}^{-1}$  and  $0.396 \text{ cm}^3\text{g}^{-1}$ , respectively. As calculated by nonlocal density functional theory (NLDFT) (Fig. 1b Inset), the COF material shows narrow pore size distribution with the dominant pore width centered around 3.0 nm, indicative of abundant mesopores in the network.

The surface morphology of **TFPT-BMTH** was further investigated by scanning electron microscopy (SEM) and transmission electron microscopy (TEM). The SEM image showed the aggregation of irregular stick-like structure (Fig. 1c). Furthermore, the TEM image revealed the porous morphology for polymer sample (Fig. 1d). EDS analyses on the same sample also confirmed the uniform distribution of the component elements of C, H, O and N within the COF material (Fig. S5, ESI<sup>†</sup>).

In the solid-state <sup>13</sup>C CP-MAS NMR spectrum of **TFPT-BMTH** (Fig. S6, ESI<sup>†</sup>), the characteristic signal at 149 ppm could be assigned to the imine groups,<sup>11,19</sup> and other signals at 56, 69, 158, and 167 ppm corresponded to 2-methoxyethoxy, triazinyl, and hydrazide groups, which are in agreement with the chemical structure of the COF material. The FT-IR spectrum of **TFPT-BMTH** showed that the characteristic stretching bands of the BMTH ( $V_{as}-NH_2$ ,  $3500 \text{ cm}^{-1}$ ;  $V_s-NH_2$ ,  $3400 \text{ cm}^{-1}$ ) and TFPT ( $HC=O$ ,  $1700 \text{ cm}^{-1}$ ) disappeared after the polycondensation reaction, clearly revealing the absence of any starting material. Meanwhile, the new stretching vibration band at  $1660 \text{ cm}^{-1}$  could be attributed to the imine linkages (Figure 2a).<sup>19</sup> The compositions were also investigated by X-ray photoelectron spectroscopy (XPS) technique (Fig. S7, ESI<sup>†</sup>). As shown in Fig. 2b, the high resolution C1s spectra showed four peaks corresponding to the C=C, C-C, C-NH and C-O bonds with bonding energy of 284.6, 285.53, 286.5 and 286.9 eV, respectively.<sup>20</sup> The high resolution N1s spectra also exhibited three peaks at 399, 400.3 and 401.3 eV, which were assigned to C-N=C, O=C-NH and C=N, respectively. The O1s spectra were deconvoluted into two bands with bonding energy of 532, 533.4 eV, corresponding to C-O and C=O bonds, respectively (Fig. S8, ESI<sup>†</sup>).<sup>21</sup>

The UV-vis diffuse reflectance spectrum of the **TFPT-BMTH** was measured to exploit the light absorption capability, and the absorption onset was found to be around 470 nm as shown in Fig. 2b. An optical band gap of 2.74 eV was calculated by the Kubeka–Munk function (Fig. 2c Inset). The **TFPT-BMTH** showed a broadened and red-shift absorption in comparison with that of its building blocks (Fig. S9, ESI<sup>†</sup>), similar to those for other COFs reported recently.<sup>22</sup> The photophysical properties of **TFPT-BMTH** was further investigated by photoluminescence spectroscopy. Upon excitation at 377 nm,

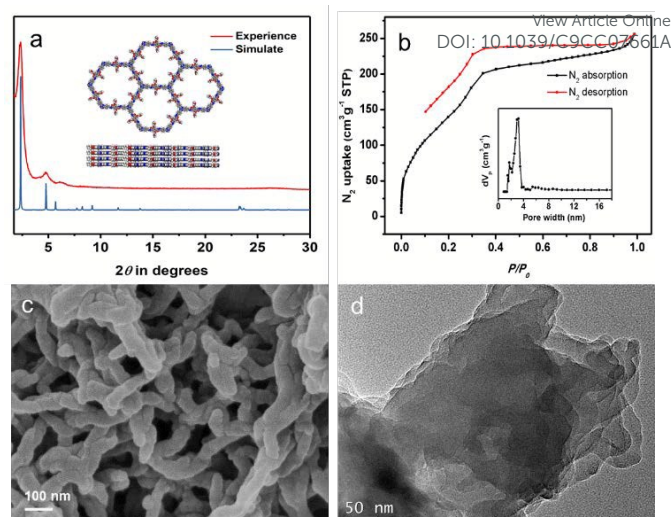


**Fig. 1** (a) Experimental and simulated PXRD patterns of **TFPT-BMTH** (Top and side views of the energy-minimized models). (b) Nitrogen sorption isotherms of **TFPT-BMTH** (inset: pore size distribution). (c) SEM image and (d) TEM image of **TFPT-BMTH**.

the COF material exhibited blue luminescence with emission maximum at 457 nm (Fig. S10, ESI<sup>†</sup>). The fluorescence quantum yield of 6.75% is comparable to those values found for some COFs.<sup>23</sup>

The fluorescence lifetime curve was shown in Fig. S11, ESI<sup>†</sup>, and the lifetime of 1.57  $\mu\text{s}$  was associated with the extended conjugated 2D structure.<sup>24</sup> The valence band (VB) of 1.68 eV was evaluated by XPS VB spectrum (Fig. 2d).<sup>20</sup> Based on the band gap (2.74 eV) obtained from UV-vis diffuse reflectance spectrum, the conduction band (CB) of **TFPT-BMTH** could be calculated to be  $-1.06 \text{ eV}$ . These values is consistent with the results measured by cyclic voltammograms (Figure S12, ESI<sup>†</sup>). The schematic band structure of **TFPT-BMTH** along with redox potentials of benzylamine (BA) and molecular oxygen was illustrated in Fig. 2e. Photoelectronic properties of **TFPT-BMTH** was investigated by transient-state photocurrent tests, and **TFPT-BMTH** generated a high photocurrent response under irradiation of visible light (Fig. 2f), revealing the available separation efficiency of photogenerated charge carriers.<sup>25</sup> Thus, the results of photophysical measurements suggested that **TFPT-BMTH** was proposed as a promising photocatalyst for visible-light-driven transformations.

Furthermore, thermogravimetric analysis (TGA) indicated that the **TFPT-BMTH** possessed a high thermal stability with minimal weight loss up to 350 °C (Fig. S13, ESI<sup>†</sup>). To explore the chemical stability, the same amount of **TFPT-BMTH** was immersed in THF, hexane,  $\text{CHCl}_3$ , toluene,  $\text{H}_2\text{O}$ , and aqueous solutions (pH = 1 and 13), respectively, at room temperature for 12 hours. The treated **TFPT-BMTH** samples were examined by PXRD (Fig. S14, ESI<sup>†</sup>) and FT-IR (Fig. S15, ESI<sup>†</sup>) techniques, and the FT-IR and PXRD analysis demonstrated that the structural integrity of the treated COF samples remained essentially unchanged, which should broaden the catalytic application under controlled conditions.

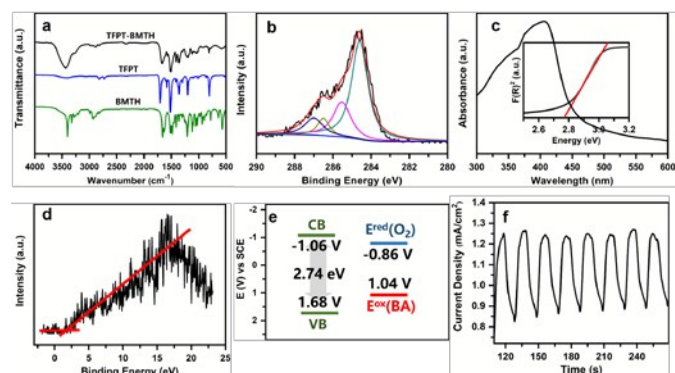


**Fig. 2** a) FT-IR spectra of **TFPT-BMTH**, **TFPT** and **BMTH**. b) XPS C1s. c) UV/Vis absorption spectrum (inset: optical band gap). d) XPS-VB. e) energy band positions of **TFPT-BMTH** together with some redox potentials. f) photocurrent tests.

The photofunctional **TFPT-BMTH** with period distribution of etheryl functional groups could be well dispersed in water, and thus the hydrophilic COF was further employed as heterogeneous catalyst to explore the visible-light-induced organic transformation in aqueous solution. The oxidative coupling reaction of benzylamine was selected as a model reaction and the optimal conditions are shown in Table S1, ES1<sup>†</sup>. To our delight, the **TFPT-BMTH** exhibited superior photocatalytic efficiency with the conversion rate of up to 99% under the investigated conditions (Table S1, entry 2, ES1<sup>†</sup>). The obtained results are evaluated by comparison with literature data obtained with other heterogeneous catalysts including other COFs (Table S2, ES1<sup>†</sup>). However, the conversion was clearly reduced to 7.5% in the absence of **TFPT-BMTH**, (Table S1, entry 6, ES1<sup>†</sup>) demonstrating that the self-coupling reaction could not efficiently proceed without catalyst. Trace conversion was observed without light irradiation, (Table S1, entry 7, ES1<sup>†</sup>), revealing the crucial role of light in the reaction. To investigate the influence of the additives on the oxidative coupling reaction of benzylamines, we carried out a series of comparative experiments by adding different scavengers into the reaction system.<sup>26</sup> when NaN<sub>3</sub> was used as a singlet oxygen scavenger (<sup>1</sup>O<sub>2</sub>), a conversion of 86% was observed (Table S1, entry 8, ES1<sup>†</sup>). while adding benzoquinone as superoxide radical (O<sub>2</sub><sup>•-</sup>) scavenger, a reduced conversion of 54% was obtained (Table S1, entry 9, ES1<sup>†</sup>), which illustrated that superoxide radical could play a more dominant role than singlet oxygen specie in the oxidative coupling reaction. After addition of EDTA(Na<sup>+</sup>) as hole scavenger under identical conditions, a conversion of only 37% was found (Table S1, Fig S16, entry 10, ES1<sup>†</sup>). Moreover, by using 2-propanol as a hydroxyl radical scavenger, the excellent conversion of 99% was achieved, indicating no effect for hydroxyl radical in catalytic process (Table S1, entry 11, ES1<sup>†</sup>). In addition, the kinetic curve of the oxidative coupling reaction was shown in Fig. S17, ES1<sup>†</sup>.

Moreover, a number of benzylamine derivatives could be employed as the substrates in the photo-oxidative coupling reaction, and the results were summarized in Table 1. The coupling reaction of 4-methyl benzylamine with electron-

**Table 1** Oxidation of benzylamine with various substituent group using **TFPT-BMTH**.<sup>a</sup> DOI: 10.1039/C9CC07661A

Entry	Substrate	Product	Conv.(%)
1			98
2			99
3			99
4			70
5			93
6			92
7			80

<sup>a</sup> Reaction conditions: **TFPT-BMTH** catalyst (5 mmol%), solvent (H<sub>2</sub>O, 5 ), benzylamine (0.2mmol), RT, 24 h, air atmosphere, blue LED (30 W, λ=454 nm).

donating group provided the benzylidene product in excellent conversion of 98% (Table 1, entry 1). The effect of substitutions on the aromatic ring of benzylamine was further investigated, and it also was found that benzylamine substrates with fluoro or chloro substituent group showed outstanding conversion (Table 1, entry 2 and 3). The 4-cyanobenzylamine exhibited the lowest reactivity among those with electron-withdrawing groups, which could be contributed to strong electron-withdrawing effect of substituent by destabilizing cationic radical intermediate (Table 1, entry 4). Interestingly, in the case of 4-methoxybenzylamine, a mixture of 4-methoxybenzaldehyde and 4-methoxybenzamide product was observed with a molar ratio of 3:1 and total conversion of 93% (Table 1, entry 5). 2-methoxybenzylamine could also be transformed into the desired imine product with a conversion of 92% (Table 1, entry 6), while 3-methoxybenzylamine exhibited a slightly lower reactivity under the identical conditions (Table 1, entry 7).

Based on our experimental results and previous literature,<sup>27</sup> a proposed mechanism on the photocatalytic oxidative coupling of benzylamines was schematically shown in Fig. S18, ES1<sup>†</sup>. Under light irradiation, **TFPT-BMTH** should excite electron from HOMO to LUMO to form the photogenerated electron-hole pairs. Then molecular O<sub>2</sub> is transformed into active oxygen species (single oxygen specie <sup>1</sup>O<sub>2</sub> and superoxide radical anion O<sub>2</sub><sup>•-</sup>) through energy or electron transfer process. Moreover, the electron paramagnetic resonance (EPR) test was performed to further verify active oxygen species (Fig. S19 and S20, ES1<sup>†</sup>). Using 5,5-Dimethyl-1-pyrroline N-oxide (DMPO)

2,2,6,6-tetramethylpiperidinyloxy (TEMPO) as active oxygen trapping agent, the characteristic signals of DMPO-O<sub>2</sub><sup>•-</sup> and TEMPO-<sup>1</sup>O<sub>2</sub> were observed in the resulting EPR spectra, which revealed that O<sub>2</sub><sup>•-</sup> and <sup>1</sup>O<sub>2</sub> involved in the photooxidative coupling of amines. Simultaneously, benzylamine is oxidized by photogenerated holes to transform into benzylamine radical cation. The reaction of the radical cation with active oxygen species to generate an hydroperoxy (phenyl)methylamine intermediate, which could convert into benzylimine after elimination of H<sub>2</sub>O<sub>2</sub>. The generated H<sub>2</sub>O<sub>2</sub> could act as an additional oxidant, and further oxidize benzylamine to produce benzylimine. Finally, the addition reaction between benzylimine intermediate and an additional benzylamine results in the desired imine product after remove of ammonia. In another path, the generated benzylimine might be hydrolyzed to benzaldehyde, which further condense with a benzylamine to form the coupling imine. Interestingly, in the oxidation of 4-methoxybenzylamine substrate, a mixture of the corresponding benzaldehyde and amide was produced, suggesting that oxidative dehydrogenation of the benzylimine intermediate led to a nitrile, followed by hydrolysis to give the resulting amide.<sup>28</sup>

The cycling test of photocatalytic oxidative coupling of amines was performed to further demonstrate the stability and reusability of **TFPT-BMTH** catalyst. As shown in Fig. S25, ESI<sup>+</sup>, the conversions in five repeating cycles were over 97%, indicating the significant reusability of **TFPT-BMTH**. After recycling reactions, the characterization results by PXRD, FT-IR, SEM and TEM (Fig. S26-S29, ESI<sup>+</sup>) also showed that the recovered samples retained its original structure and morphology. The obtained results demonstrated that **TFPT-BMTH** could be used as excellent heterogeneous catalyst with photocatalytic stability.

In summary, we have designed and synthesized a hydrophilic hydrazone-based COF **TFPT-BMTH** with high-degree integration of 2-methoxyethoxy groups on the channel walls. The hydrophilic COF material has further been employed as heterogeneous photocatalyst for oxidative coupling of benzylamines to imines, and the results have also demonstrated superior photocatalytic activity and environmentally friendly process under ambient conditions. In addition, the **TFPT-BMTH** has shown good recyclability without any substantial loss of catalytic activity. Our current protocol provides a convenient strategy to develop COFs material with high crystallinity and designed functionalities, which show potential to achieve the efficient and environmentally benign photocatalytic transformations.

The authors gratefully acknowledge financial support from the National Natural Science Foundation of China (51703076).

## Conflicts of interest

There are no conflicts to declare.

## Notes and references

- X. Feng, X. Ding, D. Jiang, *Chem. Soc. Rev.*, 2012, **41**, 6010–6022. DOI: 10.1039/C9CC07661A
- D. Stewart, D. Antypov, M. S. Dyer, M. J. Pitcher, A. P. Katsoulidis, P. A. Chater, F. Blanc, M. J. Rosseinsky, *Nat. Commun.*, 2017, **8**, 1102–1111.
- H. Furukawa, O. M. Yaghi, *J. Am. Chem. Soc.*, 2009, **131**, 8875–8883.
- Q. Gao, X. Li, G. Ning, K. Leng, B. Tian, C. Liu, W. Tang, H. Xub, K. Loh, *Chem. Commun.*, 2018, **54**, 2349–2352.
- X. Ding, J. Guo, X. Feng, Y. Honsho, J. Guo, S. Seki, P. Maitarad, A. Saeki, S. Nagase, D. Jiang, *Angew. Chem. Int. Ed.*, 2011, **50**, 1289–1293.
- C. R. DeBlase, K. E. Silberstein, T. T. Truong, H. D. Abruna, W. R. Dichtel, *J. Am. Chem. Soc.*, 2013, **135**, 16821–16824.
- T. He, K. Geng, D. Jiang, *ACS Materials Lett.*, 2019, **1**, 203–208.
- L. Chen, K. Furukawa, J. Gao, A. Nagai, T. Nakamura, Y. Dong and D. Jiang, *J. Am. Chem. Soc.*, 2014, **136**, 9806–9809.
- V. S. Vyas, F. Haase, L. Stegbauer, G. Savasci, F. Podjaski, C. Ochsenfeld, B. V. Lotsch, *Nat Commun*, 2015, **6**, 8508–8517.
- W. Liu, Q. Su, P. Ju, B. Guo, H. Zhou, G. Li, Q. Wu, *chemSusChem*, 2017, **10**, 664–669.
- L. Stegbauer, K. Schwinghammer, B. V. Lotsch, *Chem. Sci.*, 2014, **5**, 2789–2793.
- Y. F. Zhi, Z. P. Li, X. Feng, H. Xia, Y. M. Zhang, Z. Shi, Y. Mu, X. M. Liu, *J. Mater. Chem. A.*, 2017, **5**, 22933–22938.
- A. Jiménez-Almarza, A. López-Magano, L. Marzo, S. Cabrera, R. Mas-Ballesté, J. Alemán, *ChemCatChem*, 2019, **11**, 4916–4922.
- X. Wu, L. Gagliardi, D. G. Truhlar, *J. Am. Chem. Soc.*, 2018, **140**, 7904–7912.
- R. Chen, J.-L. Shi, Y. Ma, G. Lin, X. Lang, C. Wang, *Angew. Chem. Int. Ed.*, 2019, **58**, 6430–6434.
- S. Yao, S. Saaby, R. G. Hazell, K. A. Jørgensen, *Chem.-Eur. J.*, 2000, **6**, 2435–2448.
- F. J. Uribe-Romo, C. J. Doonan, H. Furukawa, K. Oisaki, O. M. Yaghi, *J. Am. Chem. Soc.*, 2011, **133**, 11478–11481.
- K. S. W. Sing, D. H. Everett, R. A. W. Haul, L. Moscou, R. A. Pierotti, J. Rouquerol, T. Siemieniowska, *Pure & Appl. Chem.*, 1985, **57**, 603–619.
- A. K. Sekizkardes, S. Altarawneh, Z. Kahveci, T. İslamoğlu, H. M. El-Kaderi, *Macromolecules.*, 2014, **47**, 8328–8334.
- P. Yang, R. Wang, M. Zhou, X. Wang, *Angew. Chem. Int. Ed.*, 2018, **57**, 8674–8677.
- H. Wang, X. Sun, D. Li, X. Zhang, S. Chen, W. Shao, Y. Tian, Y. Xie, *J. Am. Chem. Soc.*, 2017, **139**, 2468–2473.
- E. L. Spitler, W. R. Dichtel, *Nat. Chem.*, 2010, **2**, 672–677.
- Z. Li, N. Huang, K. H. Lee, Y. Feng, S. Tao, Q. Jiang, Y. Nagao, S. Irlé, D. Jiang, *J. Am. Chem. Soc.*, 2018, **140**, 12374–12377.
- J. Zhang, M. Zhang, R.-Q. Sun, X. Wang, *Angew. Chem. Int. Ed.*, 2012, **51**, 10145–10149.
- L. Lin, Z. Yu, X. Wang, *Angew. Chem. Int. Ed.*, 2019, **58**, 6164–6175.
- N. Zhang, X. Li, H. Ye, S. Chen, H. Ju, D. Liu, Y. Lin, W. Ye, C. Wang, Q. Xu, J. Zhu, L. Song, J. Jiang, Y. Xiong, *J. Am. Chem. Soc.*, 2016, **138**, 8928–8935.
- Z. J. Wang, S. Ghasimi, K. Landfester, K. A. Zhang, *Adv. Mater.*, 2015, **27**, 6265–6270.
- J. W. Kim, K. Yamaguchi, N. Mizuno, *Angew. Chem. Int. Ed.*, 2008, **47**, 9249–9251.

## A hydrophilic covalent organic framework for photocatalytic oxidation of benzylamine in water

Ziqian Liu, Qing Su,\* Pengyao Ju, Xiaodong Li, Guanghua Li, Qiaolin Wu,\* and Bing Yang\*

The hydrophilic COF exhibits superior photocatalytic activity and recyclability together with environmental benignity in photocatalytic oxidation of benzylamine in water under ambient conditions. Our approach highlights the potential of developing photofunctional COFs to achieve highly efficient and environmentally benign photocatalytic transformations.

